

EFFECTS OF TRIAXIAL AND UNIAXIAL RANDOM EXCITATION ON THE VIBRATION RESPONSE AND FATIGUE DAMAGE OF TYPICAL SPACECRAFT HARDWARE

Harry Himmelblau and Michael J. Hine
M.S. 125-129
Jet Propulsion Laboratory
California Institute of Technology
Pasadena, CA 91109-8099
(8 18)354-8564

Abraham M. Frydman
Code AMSRL-WT-PD/ALC
U.S. Army Research Laboratory
2800 Powder Mill Rd
Adelphi, MD 20783-1197
(301)394-2804

Peter A. Barrett
EER Systems, Inc.
2550 Honolulu Ave.
Montrose, CA 91020
(8 18)542-6965

Triaxial and uniaxial random vibration was applied to a typical item of aerospace equipment, and the response of certain electronic components was monitored with accelerometers to determine the relative fatigue damage between simultaneous triaxial and sequentially-applied uniaxial loading. A detailed procedure was developed to enable the comparison. In the specific case examined, triaxial excitation caused approximately twice as much damage as uniaxial excitation.

INTRODUCTION

For nearly four decades, electrodynamic shakers have been used for random vibration testing of aerospace hardware by applying uniaxial excitation even though flight data shows that the service environment is multidirectional. The difference in failure potential between sequentially-applied uniaxial testing and simultaneous multidirectional service conditions has been the subject of debate for nearly as long. Conservatism has traditionally been added to uniaxial testing, partly to compensate for this obvious deficiency, e.g., by enveloping spectral peaks in deriving vibration

criteria. Recently, important steps have been taken to reduce this conservatism, e.g., by employing force limiting in test control. Thus, the time is ripe to carefully examine the multidirectional issue.

Over the past few years, some triaxial (3-D) vibration testing has been performed, mainly on automotive equipment using a unique army facility. A test program and subsequent data analysis were performed to provide the information necessary to determine the difference in failure potential between uniaxial (1-D) and 3-D excitation for typical aerospace hardware. An item of aerospace equipment was selected as the test specimen, furnished by Hughes Space and Communications Co. The preferred method of determining the difference in failure potential is the straight-forward comparison of time-to-failure under simultaneous 3-D and sequentially-applied 1-D excitation. Unfortunately, this method would require multiple test specimens or subassembly replacement or repair, and high amplitude or long duration testing, all at considerable expense which would exceed available funds.

To avoid this situation, the following substitution was devised, namely (a) apply accelerometers to internal electronic components, (b) use the measured response under each type of excitation, (c) compute the fatigue damage, and then (d) compare the computed damage under each type of excitation (i.e., 1-D and 3-D). If the computed damage is roughly identical, it may be concluded that the results of sequentially-applied uniaxial testing is adequate for determining structural resistance to multidirectional service conditions, whereas a substantial difference in computed damage would indicate a serious deficiency in uniaxial testing. The later conclusion would form the basis for a more realistic comparison involving more costly tests to failure.

TEST SPECIMEN

The unit selected for this test program was the Hughes Ku-Band Downconverter, an equipment item used on synchronous-orbit satellites. Shown in Fig. 1 with its cover removed, this unit may be considered typical of current aerospace technology.

TEST FACILITY AND INSTRUMENTATION

Uniaxial and triaxial random vibration excitation was applied by the Triaxial Vibration Test System, located at the U.S. Army Research (formerly Harry Diamond) Laboratory, Adelphi, Maryland. This unique facility, shown in Figs. 2 and 3, was developed by Wyle Laboratories using three specially-modified Ling Model 335B electrodynamic shakers [1-2]. The test specimen was mounted to a common test table with a simple plate fixture. The excitation was controlled by a specially-designed control system developed by Synergistic Technology, Inc. [3-4].

The instrumentation was comprised of 18 accelerometers, one in each orthogonal direction (a) in the common test table for input control, and (b) mounted to four components or elements for vibration response measurements, as seen in Fig. 1. Accelerometer signals were then conditioned

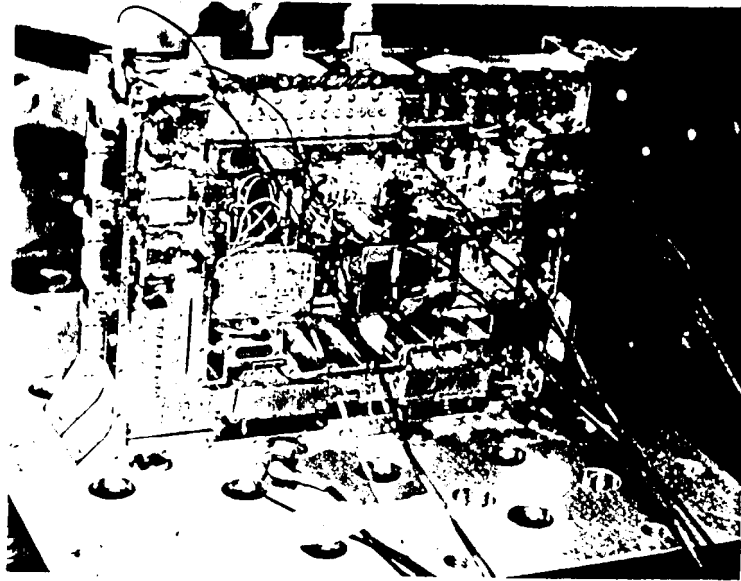


Figure 1. The Hughes Ku-band Downconverter with Cover Removed, Used as the Test Specimen. Note three accelerometers on each of four electronic components, including one component (set on the mounting plate) which failed during vibration testing.

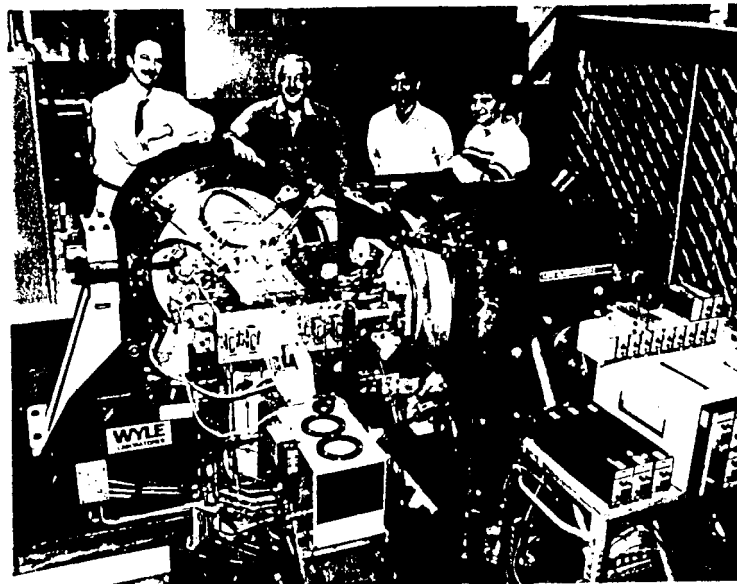


Figure 3. The Triaxial Vibration Test System with the Test Specimen and Instrumentation Installed.

with conventional charge amplifiers and recorded directly into computer memory as well as on wideband FM magnetic tape.

INPUT SPECTRUM AND DURATION

To enable the direct comparison of **uniaxial** and **triaxial** test results, the same random vibration input spectrum was utilized for the sequentially-applied **uniaxial** tests in the X, Y and Z directions, as well as the simultaneous **triaxial** test. The spectrum selected was one commonly used in the aerospace industry, namely, the minimum random vibration component acceptance spectrum of MIL-STD-1540C shown in Fig. 4 [5]. A test duration of one minute was selected “ for each **uniaxial** test as well as the **triaxial** test. Since no coherence data were available from **triaxial** flight measurements, it was assumed that the **triaxial** inputs to the shakers were incoherent (or uncorrelated) across the frequency range of interest (20-2000 Hz).

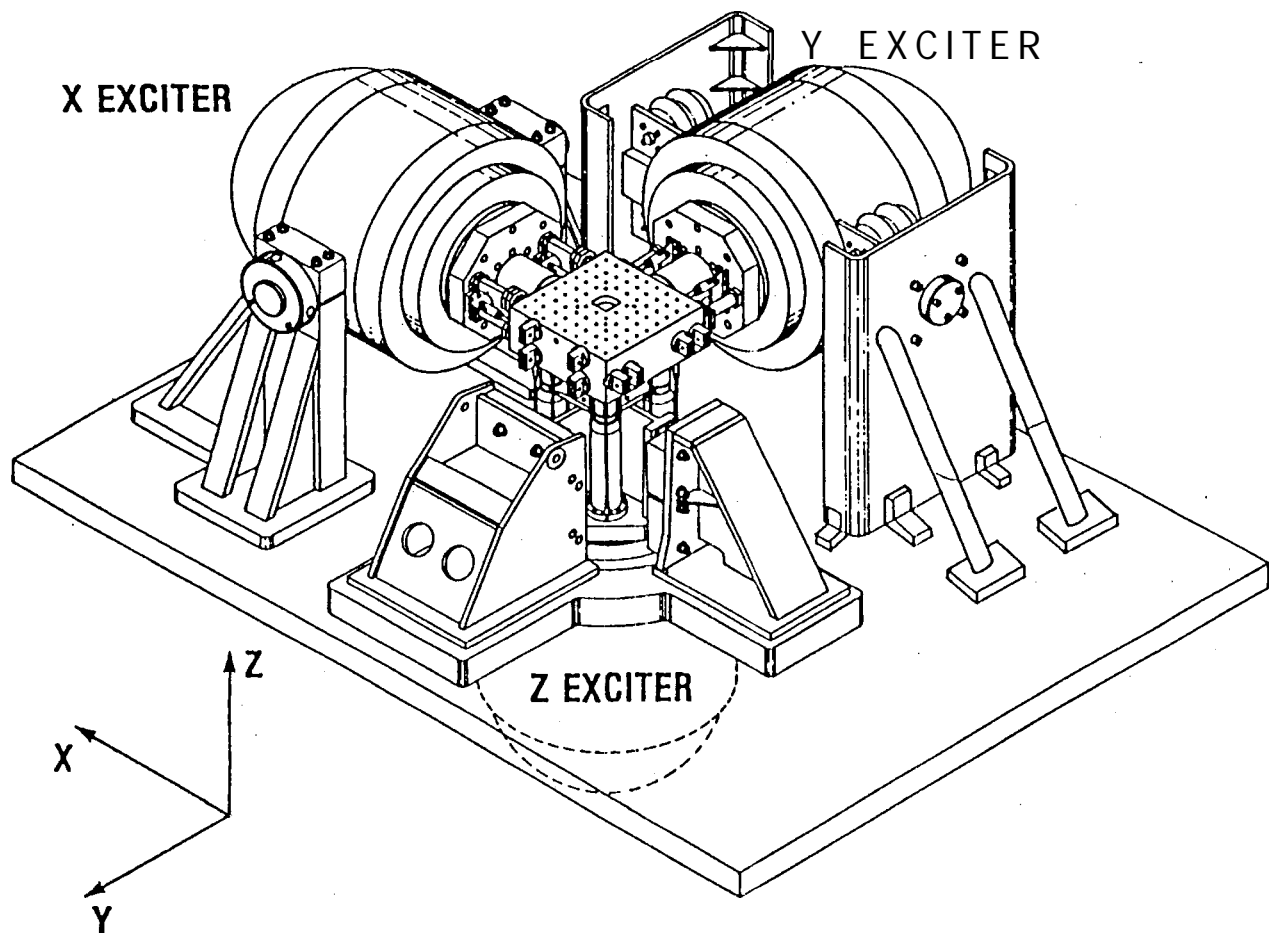


Figure 2. U. S. Army Research Laboratory Triaxial Vibration Test System.

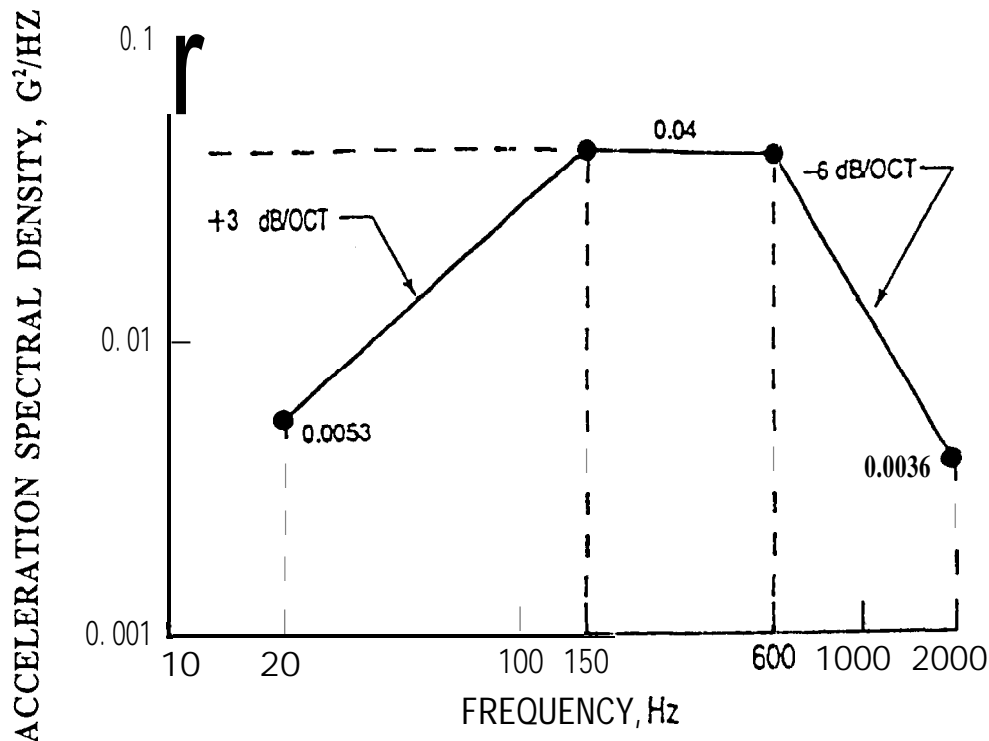


Figure 4. Minimum Random Vibration Input Acceleration Spectrum for Component Acceptance Tests from MIL-STD-1540C.

DATA PROCESSING

It has been proven that the stress response of a structure under dynamic loading is directly proportional to the velocity response [6-9]. Likewise, under random vibration, it can be shown that the stress spectrum is directly proportional to the velocity spectrum. As a consequence, it was necessary to compute the **velocity** spectrum from the acceleration spectrum, which is traditionally obtained from the recorded accelerometer signals. Figs. 5-12 show acceleration and velocity spectra for the three orthogonal accelerometers, identified as 1X, 2Y and 3Z, used to measure the response of Component A, whose location is slightly above the center of the test specimen shown in Fig. 1.

EFFECTIVE RMS VELOCITY

To utilize an S-N curve (e.g., Fig. 13) **for** determining fatigue damage under random excitation, it is necessary to (a) determine the stress from a suitably-installed strain gage, or (b) determine the effective stress from the three velocity response spectra, i.e., one spectrum in each of three orthogonal directions, for each **uniaxial** or **triaxial** excitation. In most cases, electronic components are too small to accommodate strain gages. Thus, the latter alternate was selected for this study. How the three velocity response spectra should be combined is highly dependent on their relative magnitude, coherence and phase:

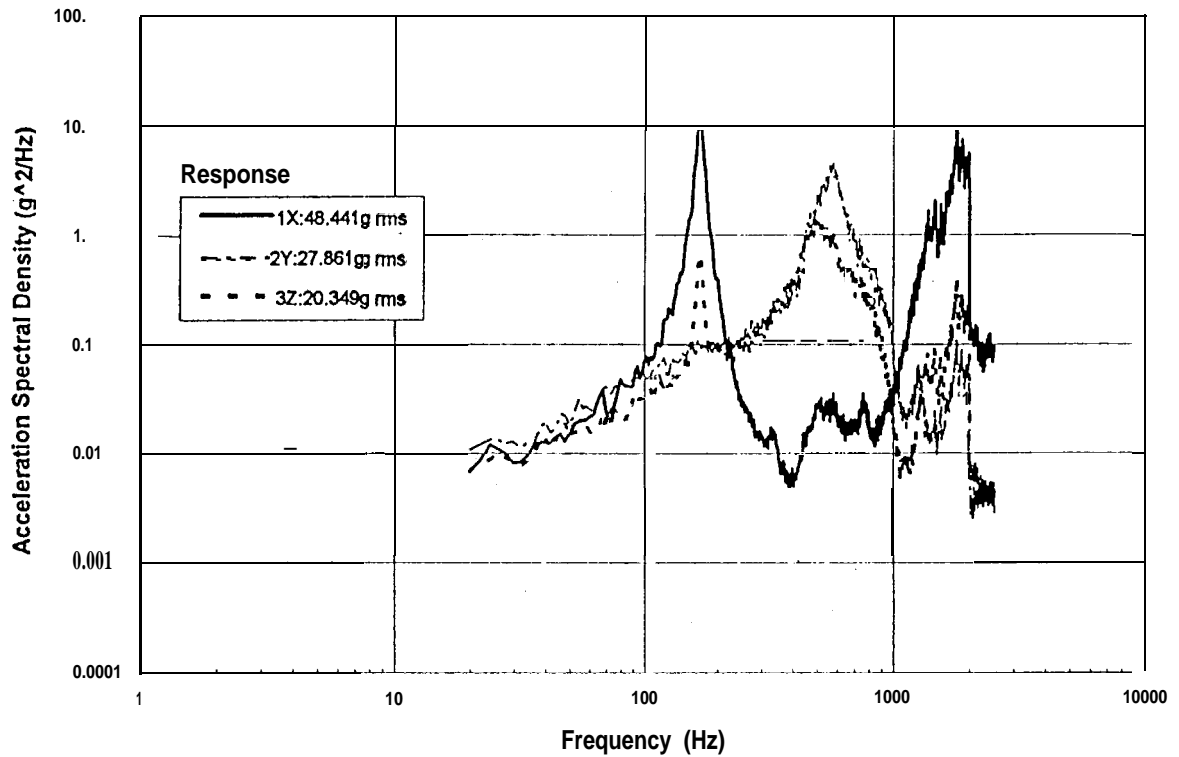


Figure 5. Acceleration Spectrum Input: XYZ-Axis, 0 dB

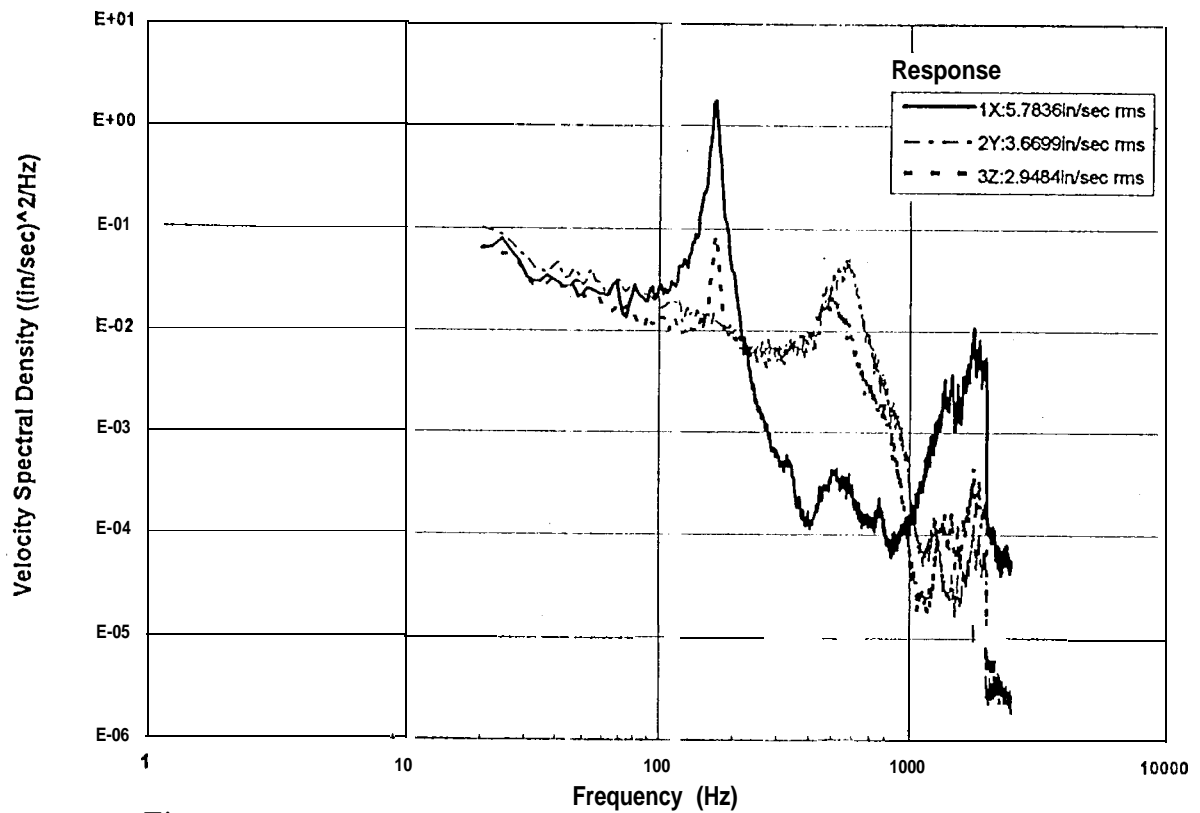


Figure 6. Velocity Spectrum Input: XYZ-Axis, 0 dB

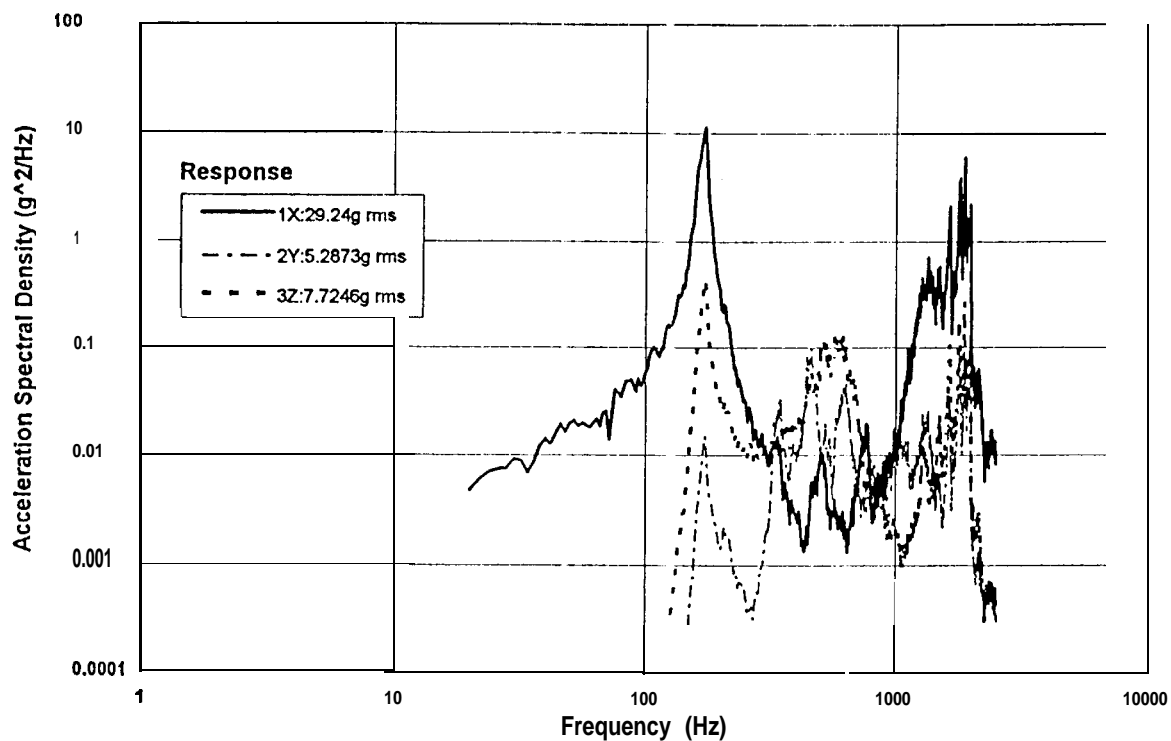


Figure 7. Acceleration Spectrum Input: X-Axis, 0 dB

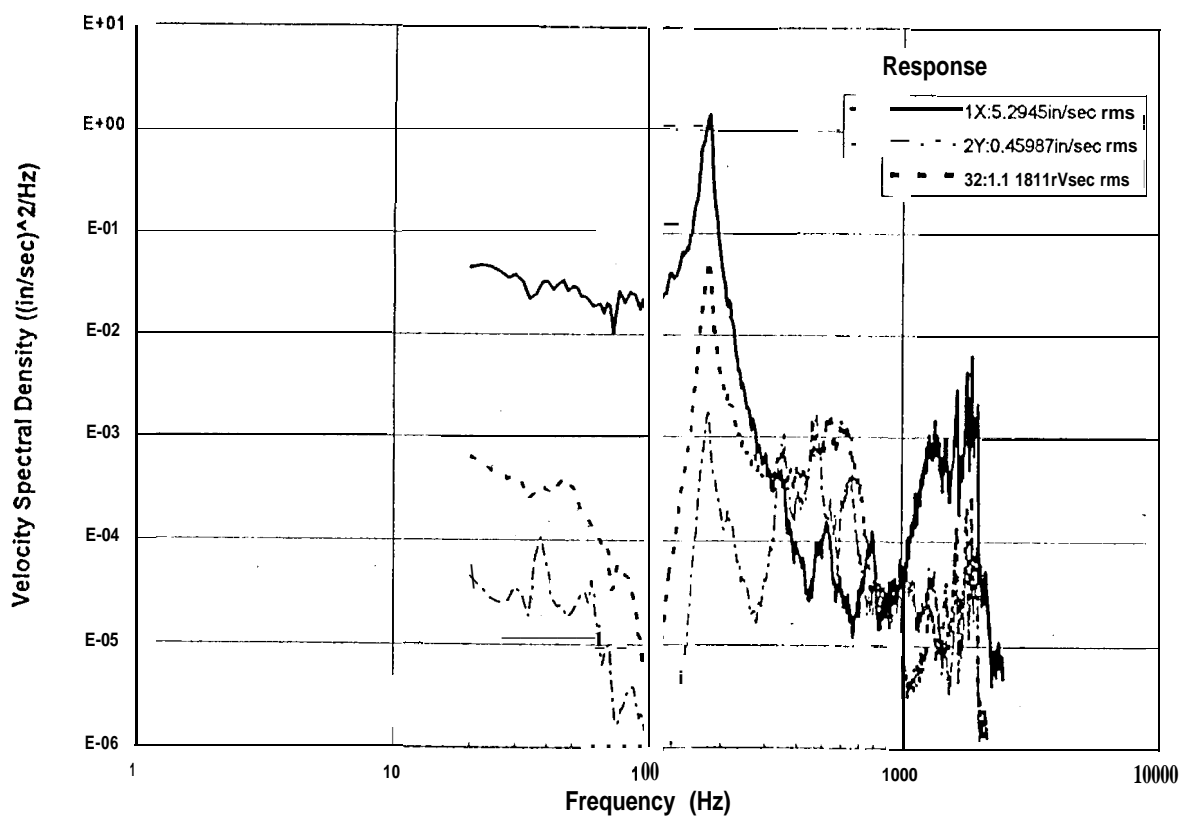


Figure 8. Velocity Spectrum input: X-Axis, 0 dB

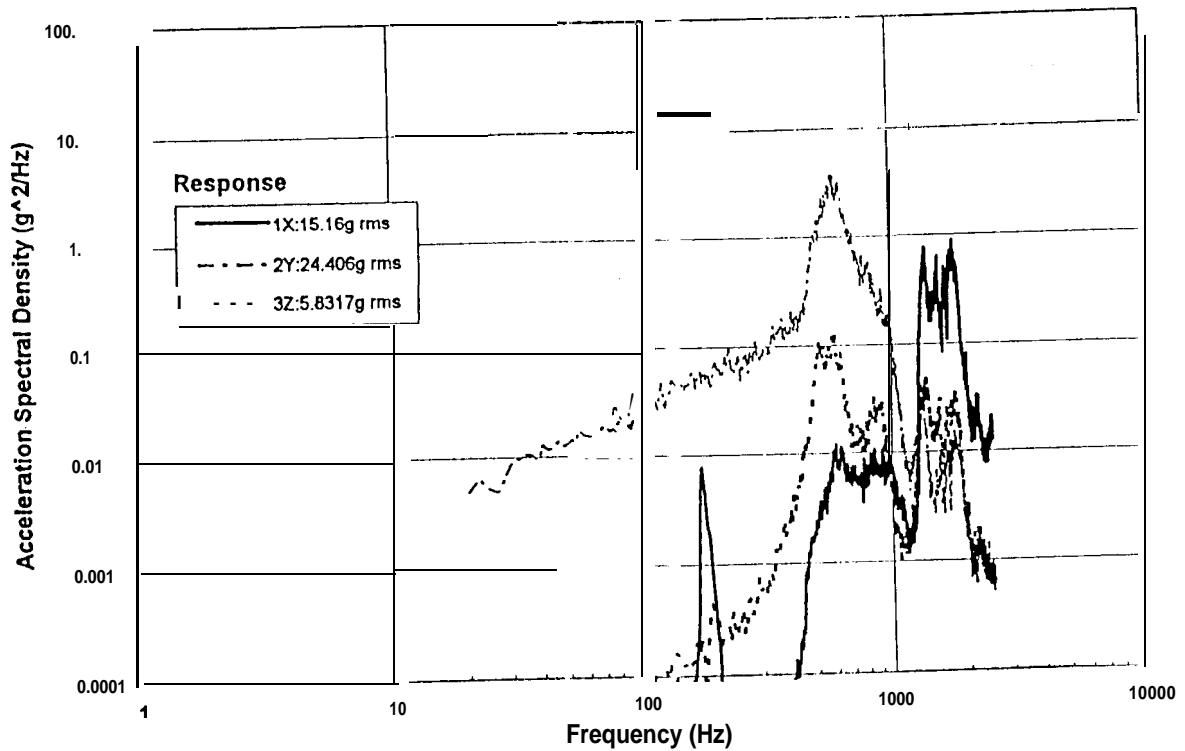


Figure 9. Acceleration Spectrum Input: Y-Axis, 0 dB

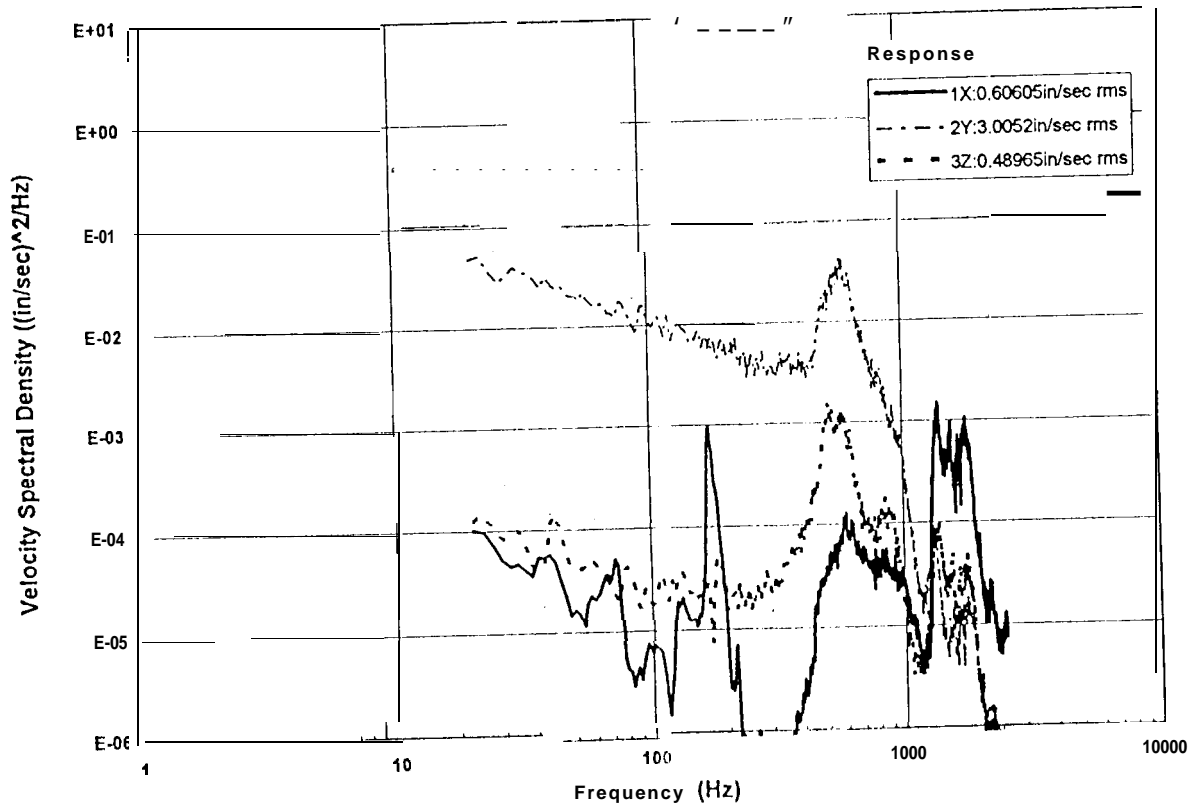


Figure 10. Velocity Spectrum Input: Y-Axis, 0 dB

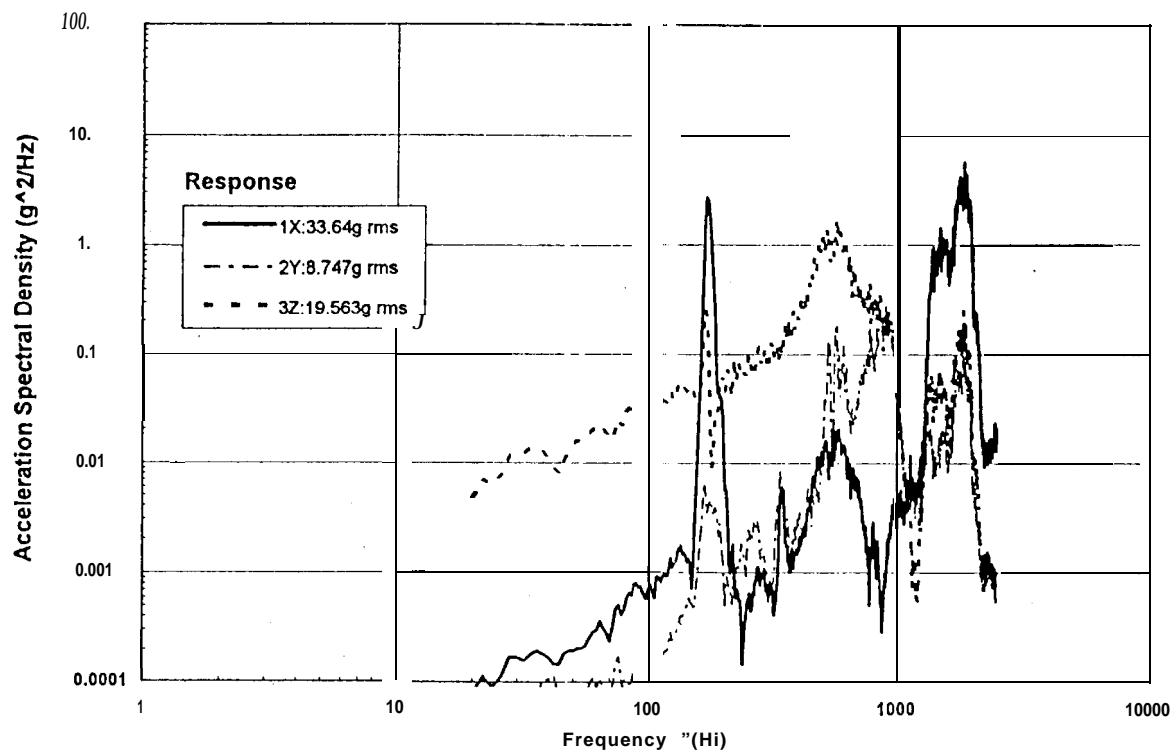


Figure 11. Acceleration Spectrum Input: Z-Axis, 0 dB

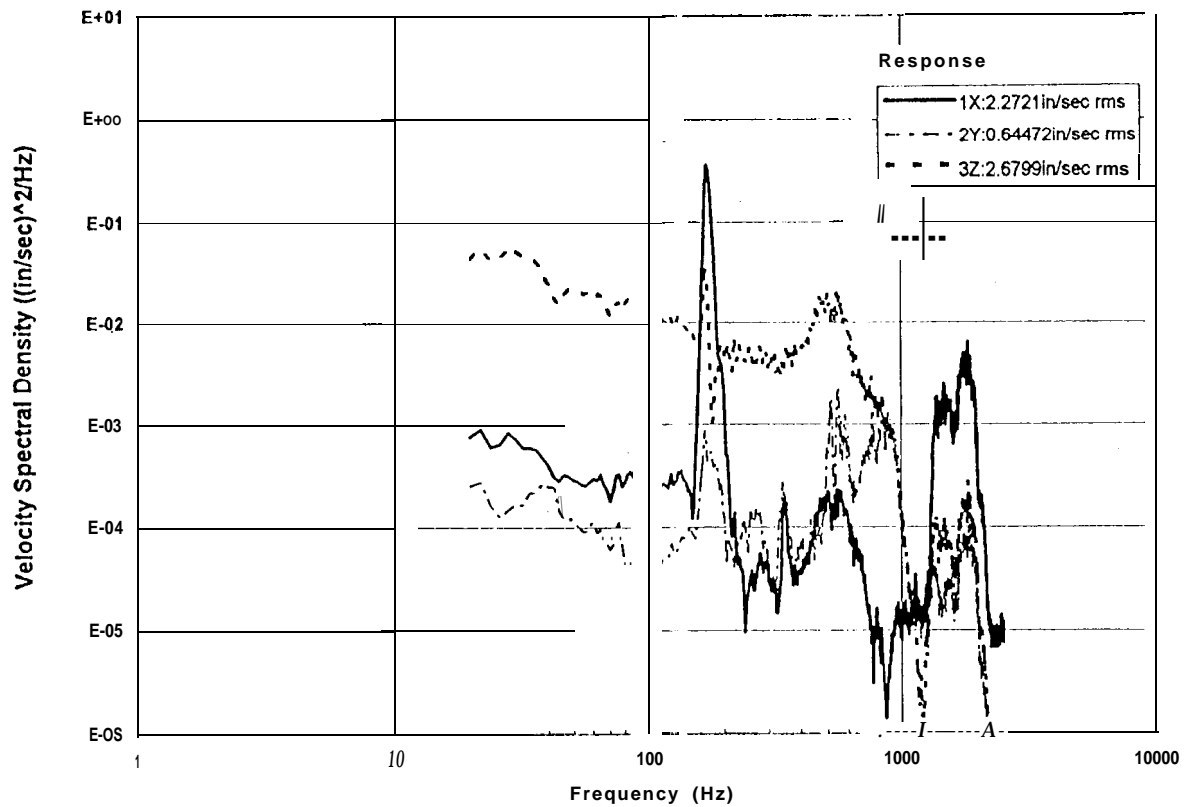


Figure 12. Velocity Spectrum Input: Z-Axis, 0 dB

- (1) If a single velocity spectrum is dominant over the other two, then only that spectrum and its rms velocity need be considered in determining the rms stress.
- (2) If two or all three velocity spectra have a significant contribution and a major percentage of these spectra show a coherence of unity and a phase angle of 0 or 180 deg., then it is necessary to relate the rms stress to the vector sum of the individual rms velocities, i.e.,

$$\sigma_{ve} = \left[\sum_{i=1}^3 (\sigma_{vi}^2) \right]^{1/2} \quad (1)$$

since the instantaneous trajectories of these velocity time histories are in phase to nearly form a straight line.

- (3) If two or all three velocity spectra have a significant contribution but are incoherent, or are coherent with phase angles other than 0 or 180 deg., the rms stress is mainly dependent on the largest velocity spectrum and rms velocity, since the instantaneous trajectories form loops (similar to hysteresis loops) with the effective stress mainly determined by the direction of the largest velocity.

TRIAxIAL RMS STRESS AND FATIGUE DAMAGE SELECTION

The objective of this study was the determination of relative fatigue damage due to sequentially-applied **uniaxial** excitation vs simultaneous **triaxial** excitation, rather than the absolute value of fatigue lives under these loadings. As a result, expensive test to failure, or finite element analysis of electronic components up to 2 k Hz, was avoided. **Thus**, it was only necessary to select an rms stress which would produce a certain amount of **fatigue** damage for a given exposure time under **uniaxial** or **triaxial** excitation. Since fatigue **damage** is a function of the number of stress cycles of the response, it was assumed under random loading that the number of stress cycles is equal to the number of zero up-crossings. In this study, it was arbitrarily decided to select an rms stress σ_{s3D} which would cause fatigue failure at the last cycle of a one minute exposure

under triaxial random excitation $\left(T_{f3D} = 60 \text{ sec} \right)$. Thus, it is assumed that the triaxial fatigue damage is $D_{3D} \equiv 1$. The S-N curve normally used for this determination should represent the material and stress concentration factor applicable to the electronic component whose response has been measured. Once this determination has been made, it is a simple matter to select the number of cycles to failure from:

$$N(\sigma_{s3D}) = \bar{f}_{3D} T_{f3D} \quad (2)$$

where the effective triaxial frequency \bar{f}_{3D} may be computed by weighting the average frequency

in each response direction $f_i (i = 1, 2, 3)$, defined as the average number of zero up-crossings per unit time, by the mean square velocity response σ_{vi} in that direction:

$$\bar{f}_{3D} = \frac{\sum_{i=1}^3 \left(f_i \sigma_{vi}^2 \right)}{\sum_{i=1}^3 \sigma_{vi}^2} \quad (3)$$

where the average frequency is [1 0-1 1]:

$$\bar{f}_i = \sigma_{ai} / 2\pi \sigma_{vi} \quad (i = 1, 2, 3) \quad (4)$$

and σ_{ai} is the rms acceleration. Once $N(\sigma_{s3D})$ is determined from Eq. (2), the effective triaxial rms stress σ_{s3D} can be obtained from the S-N curve. In addition, the ratio of stress-to-velocity should be determined from:

$$C_{3D} = \sigma_{s3D} / \sigma_{v3D} \quad (5)$$

where the effective triaxial velocity σ_{v3D} is determined by one of the three steps outlined in the prior section.

UNIAXIAL RMS STRESS AND FATIGUE DAMAGE COMPUTATIONS

The ratio of Eq. (5) may also be used to compute the uniaxial rms stresses:

$$\sigma_{sj} = C_{3D} \sigma_{vj} \quad (j = X, Y, Z) \quad (6)$$

Next, compute the number of applied cycles for each uniaxial excitation:

$$n(\sigma_{sj}) = \bar{f}_j T_{ej} \quad (7)$$

where \bar{f}_j is substituted for \bar{f}_{3D} on the LHS of Eq. (3), and T_{ej} is the exposure time for each uniaxial excitation. In this study, the exposure time T_{ej} is set equal to (T_{f3D}) i.e., $T_{ej} = 60$ sec. Then compute the number of cycles to failure for each uniaxial direction from

$$N(\sigma_{sj}) = N(\sigma_{s3D}) \left[\sigma_{s3D} / \sigma_{sj} \right]^b \quad (8)$$

where $N(\sigma_{s3D})$, σ_{s3D} and σ_{sj} are obtained from Eq. (2), the S-N curve, and Eq. (7),

respectively, and b is the fatigue exponent of the S-N curve. The fatigue exponent is a property of the material and notch geometry at the failure location, and generally varies between $4 \leq b \leq 8$.

Now, the fatigue damage from each **uniaxial** excitation can be computed using Eqs (7) and (8):

$$D_j = n(\sigma_{sj}) / N(\sigma_{sj}) \quad (9)$$

The total fatigue damage from all three uniaxial exposures is

$$D_U = \sum_{j=X}^Z D_j = D_X + D_Y + D_Z \quad (10)$$

If $D_U < 1$, it may be concluded that the total uniaxial fatigue damage is less than triaxial damage, since $D_{3D} \equiv 1$. If $D_U > 1$, failure will occur before the three uniaxial exposures are completed. Separate computations of D_X , D_Y and D_Z using Eq. (9) will indicate which uniaxial direction provides the greatest damage.

EXAMPLE

Response data for component A (located just above the center of the test specimen in Figure 1), including the acceleration and velocity response spectra presented earlier in Figs. 5-12, may be used to illustrate the fatigue damage computational procedure. The material and condition selected for this example is 2024-T3 aluminum with a theoretical stress concentration factor of 4, where sine and random S-N curves are shown in Fig. 13. For each accelerometer response measurement, the average frequency was computed using Eq. (4) and the rms acceleration and velocity values listed for each spectrum. The resulting average frequencies are tabulated in Table I.

Triaxial Excitation

Careful examination of the three velocity spectra of Fig. 6 shows that the triaxial rms velocity is controlled almost entirely by the velocity response of Accel. 1X, i.e.,

$$\sigma_{v3D} \approx \sigma_{v3D1} = 5.78 \text{ ipsrms}$$

Using the triaxial average frequencies listed in Table I, and the rms velocity listed on Fig. 6, for entry into Eq. (3):

$$f_{3D} = 515 \text{ Hz}$$

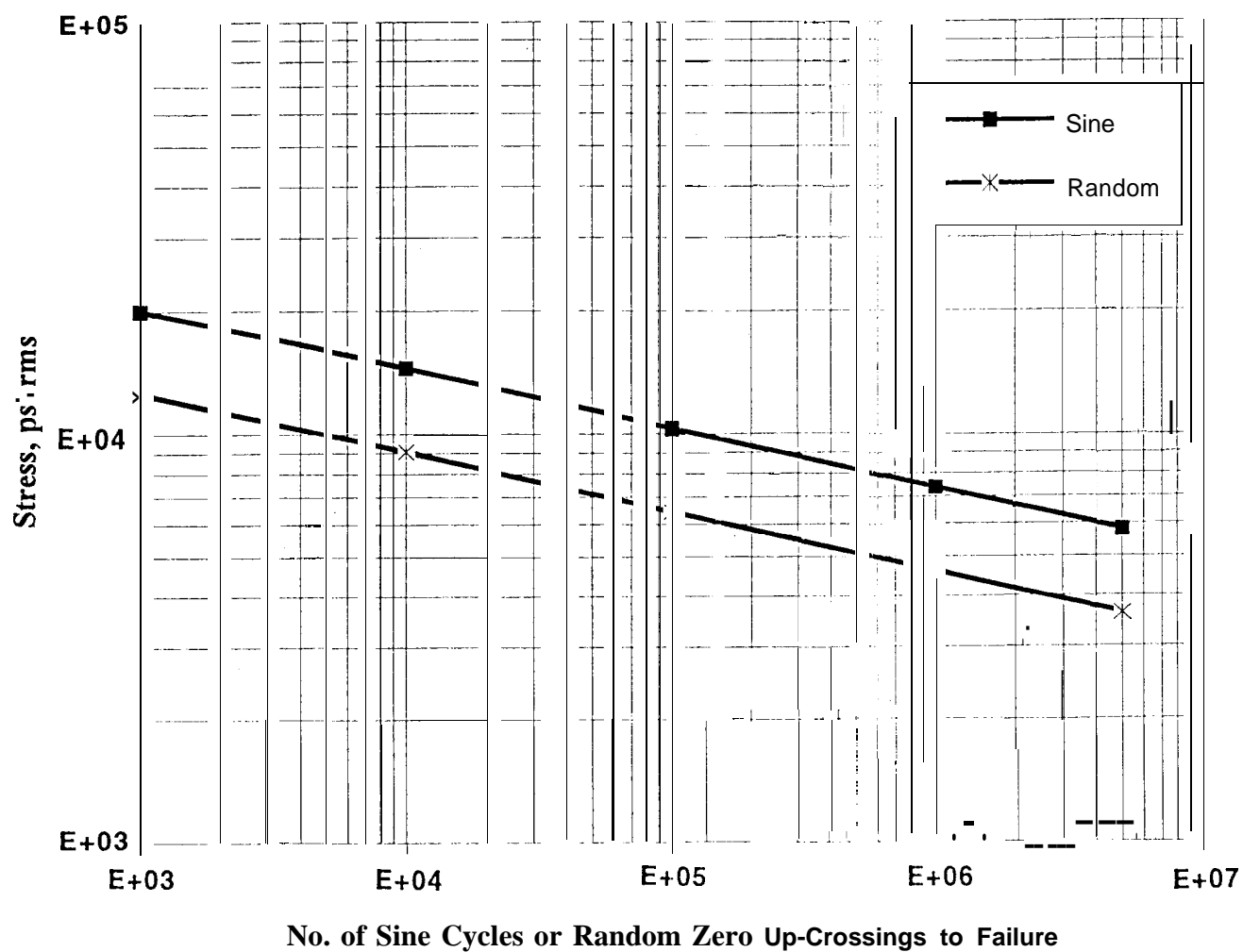


Figure 13. Sine and Random Fatigue Curves for 2024-T3 Aluminum, $K_t = 4$.

Table I. Average Frequencies for Component A Response Accelerometers

Accel No.	Excitation Direction			
	Triaxial	X- Axis	Y-Axis	Z-Axis
1X	515Hz	339Hz	1538Hz	910HZ
2Y	466	706	499	834
32	424	424	732	448

Assuming fatigue failure occurs at the end of triaxial exposure, the number of cycles to failure from Eq. (2) is:

$$N(\sigma_{s3D}) = 515 \text{ Hz} \times 60 \text{ sec} = 3.04 \times 10^4 \text{ cycles}$$

Utilizing the random S-N curve of Fig. 13, the effective triaxial stress is:

$$\sigma_{s3D} = 7600 \text{ psi rms}$$

and the stress-to-velocity ratio from Eq. (5) is:

$$C_{3D} = (7600 \text{ psi} / 5.78 \text{ ips}) = 1315 \text{ lb sec/in}^3.$$

Of course, the triaxial fatigue damage is assumed to be $D_{3D} \equiv 1$.

X-Axis Excitation

Careful examination of the three velocity response spectra of Fig. 8 shows that the X-Axis rms velocity is controlled almost entirely by Accel. 1X, i.e.,

$$\sigma_{Vx} \approx \sigma_{vX1} = 5.30 \text{ ips rms}$$

From Table I, the X-Axis average frequency is $\bar{f}_{X1} = 339 \text{ Hz}$. From Eq. (6), the X-Axis effective rms stress is:

$$\sigma_{sX} \approx \sigma_{sX1} = C_{3D} \sigma_{vX} = 1315 \times 5.30 = 7000 \text{ psi rms}.$$

From Eq. (7), the number of applied cycles in the X-Axis is:

$$n(\sigma_{sX}) = 339 \text{ Hz} \times 60 \text{ sec} = 2.04 \times 10^4 \text{ cycles}$$

Using a fatigue exponent of $b=6$, the number of cycles to failure for the X-Axis from Eq. (8) is:

$$N(\sigma_{sX}) = 3.09 \times 10^4 [7600 / 7000]^6 = 5.06 \times 10^4 \text{ cycles}$$

From Eq. (9), the X-Axis fatigue damage is therefore:

$$D_X = \left(2.04 \times 10^4 / 5.06 \times 10^4 \right)^{1/2} = 0.403.$$

Y-Axis Excitation

Careful examination of the three velocity response spectra of Fig. 10 shows that the Y-Axis rms velocity is controlled almost entirely by Accel. 2Y, i.e.,

$$\sigma_{vY} \approx \sigma_{vY2} = 3.00 \text{ ips rms}$$

Using the same procedure and example steps outlined for X-Axis excitation, the remaining Y-Axis computations are:

$$\sigma_{sY} \approx \sigma_{sY2} = 13.15 \times 3.00 = 3.950 \text{ psi rms}$$

$$n(\sigma_{sY}) = 499 \times 60 = 2.99 \times 10^4 \text{ cycles}$$

$$N(\sigma_{sY}) = 3.09 \times 10^4 [760013950]^{1/6} = 1.57 \times 10^6 \text{ cycles}$$

resulting in the Y-Axis fatigue damage:

$$D_Y = \left(2.99 \times 10^4 / 1.57 \times 10^6 \right)^{1/2} = 0.019.$$

Z-Axis Excitation

Careful examination of the three velocity response spectra of Fig. 12 shows dominant contributions from Accels 3Z and 1X. The coherence spectrum between these transducers shows unity coherence over large spectral portions. Thus, from Eq. (1):

$$\sigma_{vZ} \approx \left(\sigma_{vZ13}^2 + \sigma_{vZ1}^2 \right)^{1/2} = \left(2.68^2 + 2.27^2 \right)^{1/2} = 3.51 \text{ ips rms}$$

Using the same procedure and example steps outlined for X-Axis excitation, the remaining Z-Axis computations are:

$$\sigma_{sZ} = 13.15 \times 3.51 = 4620 \text{ psi rms}$$

$$\bar{f}_Z = \frac{448(2.68)^2 + 910(2.27)^2}{(2.68)^2 + (2.27)^2} = 641 \text{ Hz}$$

$$n(\sigma_{sZ}) = 641 \times 60 = 3.84 \times 10^4 \text{ cycles}$$

$$N(\sigma_{sZ}) = 3.09 \times 10^4 [7600/4620]^6 = 6.12 \times 10^5 \text{ cycles}$$

resulting in the Z-Axis fatigue damage:

$$D_Z = (3.84 \times 10^4 / 6.12 \times 10^5) = 0.063.$$

Cumulative Uniaxial Fatigue Damage

From Eq. (1 O), the cumulative or total uniaxial fatigue damage is the sum of the uniaxial damage contributions, i.e.,

$$D_U = D_X + D_Y + D_Z = 0.403 + 0.019 + 0.063 = 0.485.$$

which indicates that the total uniaxial damage is approximately half of the triaxial damage.

Effect of Fatigue Exponent on Total Uniaxial Damage

The fatigue exponent has long been recognized as having a major influence on cumulative fatigue damage. It was therefore decided to program other values of b into the above example computations. The results of varying the exponent between $4 \leq b \leq 8$ are tabulated in Table II and graphed in Fig. 14. This figure shows that the total uniaxial fatigue damage varies between approximately 0.75 and 0.40, with the damage varying inversely with the exponent as anticipated.

CONCLUSION

It has been demonstrated that fatigue damage under simultaneous triaxial random excitation was nearly twice the damage from sequentially-applied uniaxial excitation, based on vibration testing of typical aerospace hardware, a given set of accelerometer response measurements, a fatigue exponent of six, equal uniaxial and triaxial exposure times, and the foregoing computational procedure.

Table II. Uniaxial Fatigue Damage Computation

Fatigue Exponent	Excitation Direction	RMS Stress	No. Applied Cycles	Cycles To Failure	Directional Damage	Total Damage
b	j	σ_{sj}	$n(\sigma_{sj})$	$N(\sigma_{sj})$	D_j	D_U
4	x	7000	20400	42936	0.475	0.715
	Y	3945	29900	425623	0.070	
	z	4620	38400	226279	0.170	
5	x	7000	20400	46616	0.438	0.577
	Y	3945	29900	819958	0.036	
	z	4620	38400	372234	0.103	
6	X	7000	20400	50612	0.403	0.485
	Y	3945	29900	1579640	0.019	
	Z	4620	38400	612334	0.063	
7	X	7000	20400	54950	0.371	0.419
	Y	3945	29900	3043158	0.010	
	Z	4620	38400	1007302	0.038	
8	X	7000	20400	59660	0.342	0.370
	Y	3945	29900	5862612	0.005	
	Z	4620	38400	1657034	0.023	

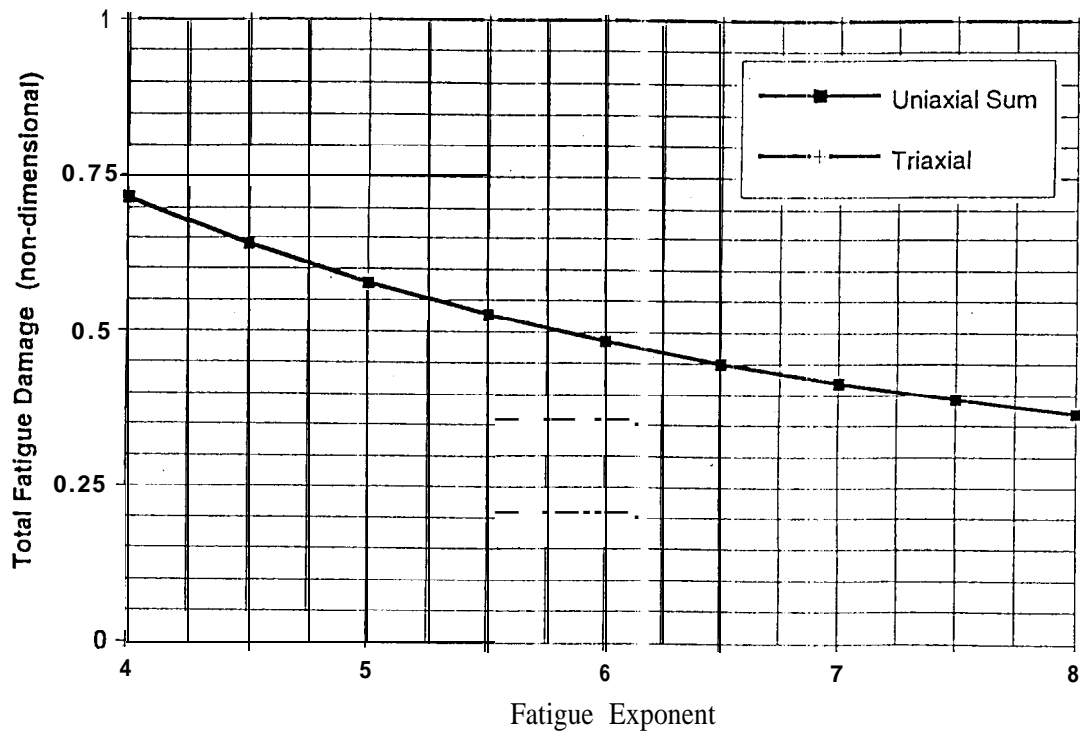


Figure 14. Fatigue Damage due to Random Vibration Testing of Component A.

ACKNOWLEDGEMENTS

The research described in this study was carried out at the Jet Propulsion Laboratory, California Institute of Technology **and** at the U.S. Army Research Laboratory, under a contract with the National Aeronautics and Space Administration. The authors express their appreciation to the following individuals for their contributions to this study: H. M. Davidson, E. A. Szymanski, T. H. Li and M. Berman of the Army Research Laboratory; W. F. Davis of Hughes Space and Communications Company; A. G. Piersol of Piersol Engineering Company; D. L. Kern, M. Gibbel, **S. L. Cornford**, D. W. Lewis and N. DuBarry of the Jet Propulsion Laboratory.

Special appreciation is expressed to Code QT, NASA Headquarters, for their sponsorship of this study under their Test Effectiveness Program.

REFERENCES

1. Frydman, A. M. and Cappel, K. L., 1985, "3-Dimensions Vibration Test System", Presented at *31st ATM, Inst. Envir. Se.*, Apr./May.
2. Freeman, M. T., "3-axis vibration test system simulates real world", *Test Engineering and Management*, 1990/1991, v. 52, v. 6, pp 10-14, Dec. /Jan.
3. Hamma, G. A. and Stroud, R. C., "Closed-Loop Digital Control of Multiaxis Vibration Testing", *Proc., 31st ATM, Inst. Envir. Se.*, 1985, pp 501-506, Apr./May.
4. Stroud, R. C. and Hamma, G. A., "Multiexciter and Multiaxis Vibration Exciter Control Systems", *Sound and Vibration*, **1988**, v. 22, n.4, pp 18-28, Apr.
5. Anon., "Test Requirements for Launch, Upper-Stage, and Space Vehicles", *Military Standard MIL-STD-1540C*, 1994, Figure 5, p. 77, Sept. 15.
6. Hunt, F. V., "Stress and Strain Limits on the Attainable Velocity in Mechanical Vibration", *J. Acoust. Soc. Amer.*, 1960, v.32, n. 9, pp 1123-1128, Sept.
7. Ungar, E. E., "Maximum Stresses in Beams and Plates Vibrating at Resonance", *Trans. ASME, J. Engrg Ind.*, 1962, v. 82B, n.1, pp 149-155, Feb.
8. Crandall, S. H., "Relation between Strain and Velocity in Resonant Vibration", *J. Acoust. Soc. Amer.*, 1962, v. 34, n. 12, pp 1960-1961, Dec.
9. Gaberson, H. A. and Chalmers, R. H., "Modal Velocity as a Criterion of Shock Severity", *Shock and Vibration Bull.* 40, Pt 2, 1969, pp 31-49, Dec.
10. Rice, S. O., "Mathematical Analysis of Random Noise", *Bell Sys. Tech. J.*, 1945, v. 24, p. 60,
11. Wax, N., Ed., *Selected Papers on Noise and Stochastic Processes*, 1954, p. 192, Dover Publ., Mineola, NY,